

See discussions, stats, and author profiles for this publication at: <https://www.researchgate.net/publication/26234674>

# NMR Detected Hydrogen–Deuterium Exchange Reveals Differential Dynamics of Antibiotic- and Nucleotide–Bound Aminoglycoside Phosphotransferase 3'-IIIa

ARTICLE *in* JOURNAL OF THE AMERICAN CHEMICAL SOCIETY · JULY 2009

Impact Factor: 12.11 · DOI: 10.1021/ja901685h · Source: PubMed

---

CITATIONS

16

READS

19

---

## 2 AUTHORS, INCLUDING:



Engin H. Serpersu

University of Tennessee

84 PUBLICATIONS 1,730 CITATIONS

SEE PROFILE

## NMR Detected Hydrogen–Deuterium Exchange Reveals Differential Dynamics of Antibiotic- and Nucleotide-Bound Aminoglycoside Phosphotransferase 3'-IIIa

Adrienne L. Norris<sup>†</sup> and Engin H. Serpersu<sup>\*,†,‡,§</sup>

Department of Biochemistry and Cellular and Molecular Biology, The University of Tennessee, Knoxville, Tennessee, 37996, Graduate School of Genome Science and Technology, University of Tennessee and Oak Ridge National Laboratories, Knoxville, Tennessee 37996, and Bioscience Division, Oak Ridge National Laboratory, Oak Ridge, Tennessee

Received March 4, 2009; E-mail: Serpersu@utk.edu

**Abstract:** In this work, hydrogen–deuterium exchange detected by NMR spectroscopy is used to determine the dynamic properties of the aminoglycoside phosphotransferase 3'-IIIa (APH), a protein of intense interest due to its involvement in conferring antibiotic resistance to both Gram negative and Gram positive microorganisms. This represents the first characterization of dynamic properties of an aminoglycoside-modifying enzyme. Herein we describe *in vitro* dynamics of apo, binary, and ternary complexes of APH with kanamycin A, neomycin B, and metal–nucleotide. Regions of APH in different complexes that are superimposable in crystal structures show remarkably different dynamic behavior. A complete exchange of backbone amides is observed within the first 15 h of exposure to D<sub>2</sub>O in the apo form of this 31 kDa protein. Binding of aminoglycosides to the enzyme induces significant protection against exchange, and ~30% of the amides remain unexchanged up to 95 h after exposure to D<sub>2</sub>O. Our data also indicate that neomycin creates greater solvent protection and overall enhanced structural stability to APH than kanamycin. Surprisingly, nucleotide binding to the enzyme–aminoglycoside complex increases solvent accessibility of a number of amides and is responsible for destabilization of a nearby  $\beta$ -sheet, thus providing a rational explanation for previously observed global thermodynamic parameters. Our data also provide a molecular basis for broad substrate selectivity of APH.

### Introduction

Aminoglycoside-modifying enzymes are employed by various Gram negative and Gram positive pathogenic bacteria for the purpose of detoxifying aminoglycoside antibiotics. This class of antibiotics is among several in clinical use that have significantly lost their effectiveness in recent decades due to the presence of bacterial proteins capable of catalyzing a drug-modifying event. Many of these have been shown to be highly promiscuous.<sup>1–4</sup> The aminoglycoside phosphotransferase (3')-IIIa (APH) is one such enzyme<sup>5,6</sup> found in *Enterococcal* and

*Staphylococcal* bacterial strains<sup>7</sup> that can detoxify more than 10 different aminoglycosides of various size and structure by transferring a phosphate group from ATP to the 3' and/or 5" hydroxyl group.<sup>8</sup> Such modifications greatly decrease the antibiotic's affinity for the 30S ribosome where it normally would bind and prevent proper protein translation in the bacterium, leading to cell death. Because of its broad substrate selectivity, APH has been extensively studied by kinetic and thermodynamic means as a model for aminoglycoside-modifying enzymes and other proteins with large ligand repertoires.<sup>6,8–13</sup> Crystal structures of APH in various binary and ternary complexes have also been solved in recent years.<sup>14,15</sup> A wealth of global information about APH and its target interactions has

<sup>†</sup> Department of Biochemistry and Cellular and Molecular Biology, The University of Tennessee.

<sup>‡</sup> Graduate School of Genome Science and Technology, University of Tennessee and Oak Ridge National Laboratories.

<sup>§</sup> Biosciences Division, Oak Ridge National Laboratory.

<sup>1</sup> Abbreviations: HD; hydrogen–deuterium, APH; aminoglycoside phosphotransferase (3')-IIIa, HSQC; Heteronuclear Single Quantum Coherence (H<sub>2</sub>O and D<sub>2</sub>O subscripts represent the respective solvent), SOFAST-HMQC; band-Selective Optimized-Flip-Angle Short-Temporary Heteronuclear Multiple Quantum Coherence, DTT; Dithiothreitol, HEPES; 4-(2-hydroxyethyl)-1-piperazineethanesulfonic acid, AMPPCP;  $\beta$ - $\gamma$ -methylene adenosine 5'-triphosphate.

- (1) Wright, E.; Serpersu, E. H. *Biochemistry* **2005**, *44*, 11581–11591.
- (2) Shaw, K. J.; Rather, P. N.; Hare, R. S.; Miller, G. H. *Microbiol. Rev.* **1993**, *57*, 138–163.
- (3) Gates, C. A.; Northrop, D. B. *Biochemistry* **1988**, *27*, 3820–3825.
- (4) Hedge, S. S.; Dam, T. K.; Brewer, C. F.; Blanchard, J. S. *Biochemistry* **2002**, *41*, 7519–7527.
- (5) McKay, G. A.; Thompson, P. R.; Wright, G. D. *Biochemistry* **1994**, *33*, 6936–6944.

- (6) Ozen, C.; Serpersu, E. H. *Biochemistry* **2004**, *43*, 14667–14675.
- (7) Howe, R. A.; Brown, N. M.; Spencer, R. C. *J. Clin. Pathol.* **1996**, *49*, 444–449.
- (8) Boehr, D. D.; Thompson, P. R.; Wright, G. D. *J. Biol. Chem.* **2001**, *276*, 23929–23936.
- (9) McKay, G. A.; Wright, G. D. *J. Biol. Chem.* **1995**, *270*, 24686–24692.
- (10) Ozen, C.; Malek, J. M.; Serpersu, E. H. *J. Am. Chem. Soc.* **2006**, *128*, 15248–15254.
- (11) Ozen, C.; Norris, A. L.; Land, M. L.; Tjioe, E.; Serpersu, E. H. *Biochemistry* **2008**, *47*, 40–49.
- (12) Thompson, P. R.; Hughes, D. W.; Wright, G. D. *Biochemistry* **1996**, *35*, 8686–8695.
- (13) Thompson, P. R.; Schwartzenhauer, J.; Hughes, D. W.; Berghuis, A. M.; Wright, G. D. *J. Biol. Chem.* **1999**, *274*, 30697–30706.
- (14) Burk, D. L.; Hon, W. C.; Leung, A. K.-W.; Berghuis, A. M. *Biochemistry* **2001**, *40*, 8756–8764.
- (15) Fong, D. H.; Berghuis, A. M. *EMBO J.* **2002**, *21*, 2323–2331.

been gleaned from these studies; however, the molecular basis of substrate promiscuity and selection patterns of APH or any other aminoglycoside-modifying enzyme remains unknown. In this work, we report the first analysis of dynamic behavior of an aminoglycoside-modifying enzyme and provide a site-specific look into the intricacies of antibiotic and nucleotide binding. Our data highlight remarkable differences between the global dynamic properties of the apo- and the ligand-bound forms of the enzyme and also reveal the structural consequences of antibiotic and nucleotide binding in a residue-specific manner. Moreover, our results provide an explanation for the significant differences observed in the global thermodynamic parameters of complexes of enzyme with aminoglycosides in the absence and the presence of metal-ATP and reveal regions of the enzyme that contribute to these differences.

## Materials and Methods

**Chemicals.** From Cambridge Isotope Laboratories (Andover, MA) were purchased 99.9% deuterium oxide and 99%  $^{15}\text{N}$  enriched salts. Dithiothreitol (DTT) was acquired from Inalco Spa (Milano, Italy), while aminoglycosides and all other chemicals were obtained in the highest possible purity from Sigma-Aldrich.

**Enzyme Purification.** APH was isolated from cells grown in  $^{15}\text{N}$ -enriched minimal media and purified as described earlier.<sup>5,6</sup> Triple-labeled APH ( $^{15}\text{N}, ^{13}\text{C}, ^2\text{H}$ -APH) was isolated from cells grown in minimal media using  $^{13}\text{C}, ^2\text{H}$ -glucose and  $^{15}\text{N}$ -salts. 10 mM DTT was maintained at all times to keep the enzyme in a monomeric state due to the well-known tendency of this protein to dimerize via disulfide bond formation<sup>5</sup> which alters its substrate binding properties.<sup>10</sup>

**Nuclear Magnetic Resonance.** NMR samples used in resonance assignments contained 250  $\mu\text{M}$   $^{15}\text{N}, ^{13}\text{C}, ^2\text{H}$ -APH and 300  $\mu\text{M}$  tobramycin in 50 mM 4-(2-hydroxyethyl)-1-piperazineethanesulfonic acid (HEPES) and 50 mM NaCl, pH 7.5. Three-dimensional HNCA, HNCACB spectra were acquired on a 900 MHz Varian spectrometer in the Complex Carbohydrate Research Center of the University of Georgia. HNCO, HNCOCA, HNCOC-CH, and  $^{15}\text{N}-^1\text{H}$  heteronuclear single quantum coherence (HSQC) [ $\text{H}_2\text{O}$  and  $\text{D}_2\text{O}$  subscripts represent the respective solvent] spectra were acquired with a 600 MHz Varian spectrometer at the University of Tennessee. The resonance assignments of the enzyme will be published elsewhere after their completion. A table of partial assignments and the  $^1\text{H}-^{15}\text{N}$  HSQC spectrum used in assignments is provided in the Supporting Information. We note that several missing assignments do not affect the conclusions of this work.

In hydrogen-deuterium (HD) exchange experiments, APH was present at 250  $\mu\text{M}$  concentration in 50 mM HEPES and 50 mM NaCl, pH 7.5. Where applicable, concentrations of kanamycin A, neomycin B (henceforth will be referred simply as kanamycin and neomycin, respectively),  $\beta-\gamma$ -methylene adenosine 5'-triphosphate (AMPPCP), and MgCl<sub>2</sub> used were 300, 350, 500, and 1000  $\mu\text{M}$ , respectively, ensuring >91% binding site saturation as calculated from previously determined dissociation constants.<sup>6,16</sup> HD exchange was followed by successive acquisition of  $^{15}\text{N}-^1\text{H}$  correlation spectra in samples immediately after dissolving them in D<sub>2</sub>O. Initial experiments indicated that a large number of amides may be exchanging very rapidly. Therefore, two sets of spectra were acquired with matched samples. Band-selective optimized-flip-angle short-transient heteronuclear multiple quantum coherence (SOFAST HMQC)<sup>17</sup> experiments were employed to acquire more frequent data points at early stages of the exchange while sensitivity

enhanced  $^{15}\text{N}-^1\text{H}$  HSQC<sup>18</sup> with TROSY option<sup>19</sup> was acquired to collect data up to 95 h of exchange. HSQC experiments yielded spectra with better resolution compared to SOFAST HMQC. Excellent agreement between the two sets of data acquired for all complexes confirmed validity and reproducibility of the observed HD exchange patterns.

SOFAST experiments were optimized to a tip angle of 120 degrees (8.4  $\mu\text{s}$ ) and a delay of 300 ms between the scans while HSQC data was collected with 1 s delays. Experiments in H<sub>2</sub>O were conducted with 48–64 transients of 2048 real data points and 80 t<sub>1</sub> increments in the nitrogen dimension. For D<sub>2</sub>O exchange, it was necessary to collect spectra quickly with as little resolution sacrifice as possible. To this end, 16 scans were collected for 2048 real data points while second dimension increments were decreased to 48. Spectral widths were held at 8012 and 2500 Hz for the  $^1\text{H}$  and  $^{15}\text{N}$  dimensions, respectively. A series of spectra were acquired after hydration of lyophilized samples in D<sub>2</sub>O at various time intervals up to 7 h in SOFAST HMQC and up to 95 h in HSQC experiments. The time between the dissolution of lyophilized samples in D<sub>2</sub>O and the start of the data acquisition varied between 3 and 3.5 min. All experiments were performed at 27 °C to optimize the quantity of observable peaks with the stability of the protein. For a few samples, a HSQC spectrum was taken in H<sub>2</sub>O before and after D<sub>2</sub>O exchange to ensure structural integrity of the lyophilized enzyme with and without ligands. In addition, no loss of enzymatic activity was observed during the experimental process.

All data were processed in identical fashion with nmrPipe software<sup>20</sup> where a sin window function was applied in both dimensions and the left half of the proton spectrum was taken. For the  $^{15}\text{N}$  dimension, spectra were zero filled to 256 points. No baseline correction or other cosmetic procedures were applied. Data were analyzed with Sparky (T. D. Goddard and D. G. Kneller, SPARKY 3, University of California, San Francisco) at matching contour levels. Protein structures were displayed with YASARA<sup>21</sup> software.

Rates of hydrogen exchange were calculated from the exponential decay of peak intensity versus time plots for individual residues and corrected for temperature and neighbor blocking/inducing effects as described elsewhere.<sup>22–24</sup> Briefly, protection factors were calculated as  $P = k_{\text{rc}}/k_{\text{obs}}$  where  $k_{\text{rc}}$  is the corrected rate of exchange calculated for the amino acid in a random coil (completely exposed to solvent) from model peptides<sup>22,24</sup> and  $k_{\text{obs}}$  is the observed rate of exchange derived from exponential peak intensity decay curves.  $\Delta G_{\text{ex}}$  values were determined from the relationship,  $\Delta G_{\text{ex}} = -RT \ln K_{\text{ex}}$ , where  $K_{\text{ex}} = k_{\text{obs}}/k_{\text{rc}}$ . A list of calculated protection factors and derived thermodynamic parameters are listed in Table 1. Upon data analysis, it was discovered that the earlier time points collected by SOFAST contained only slightly more peaks than the first HSQC HD spectrum further emphasizing the incredible dynamic behavior of this enzyme. For simplicity, the text will refer to all data as HSQC henceforth.

## Results

**Apo- and Holo-APH.** As reported earlier,<sup>16</sup> and as shown in Figure 1A, the HSQC<sub>H2O</sub> spectrum of APH in the absence of any ligands shows an extensively overlapped pattern of cross-

- (16) Welch, K. T.; Virga, K. G.; Whittemore, N. A.; Ozen, C.; Wright, E.; Brown, C. L.; Lee, R. E.; Serpersu, E. H. *Bioorg. Med. Chem.* **2005**, 13, 6252–6263.
- (17) Schanda, P.; Kupce, E.; Brutscher, B. *J. Biomol. NMR* **2005**, 33, 199–211.

- (18) Kay, L. E.; Keifer, P.; Saarinen, T. *J. Am. Chem. Soc.* **1992**, 114, 10663–10665.
- (19) Pervushin, K.; Riek, R.; Wider, G.; Wuthrich, K. *Proc. Natl. Acad. Sci. U.S.A.* **1997**, 94, 12366–12371.
- (20) Delaglio, F.; Grzesiek, S.; Vuister, G. W.; Zhu, G.; Pfeifer, J.; Bax, A. *J. Biomol. NMR* **1995**, 6, 277–293.
- (21) Krieger, E.; Koraimann, G.; Vriend, G. *Proteins* **2002**, 47, 393–402.
- (22) Bai, Y. W.; Milne, J. S.; Mayne, L.; Englander, S. W. *Proteins* **1993**, 17, 75–86.
- (23) Englander, S. W.; Kallenbach, N. R. *Q. Rev. Biophys.* **1983**, 16, 521–655.
- (24) Molday, R. S.; Englander, S. W.; Kallen, R. G. *Biochemistry* **1972**, 11, 150–158.

**Table 1.** Protection Factors ( $P$ ) and Free Energies of Exchange ( $\Delta G_{\text{ex}}$ ) Values for Residues That Are in the Intermediary Exchange Regime and Shared between the Complexes<sup>a</sup>

residue	APH-Kanamycin		APH-Neomycin	
	$P$ ( $\times 10^3$ )	$\Delta G_{\text{ex}}$ (kcal/mol)	$P$ ( $\times 10^3$ )	$\Delta G_{\text{ex}}$ (kcal/mol)
Gly 213	80.6 ± 16.2	6.73 ± 1.35	166 ± 28.7	7.16 ± 1.24
Ile 6	48.9 ± 4.29	6.44 ± 0.56	unexchanged	unexchanged
Ile 247	9.10 ± 2.38	5.43 ± 1.43	14.5 ± 5.59	5.71 ± 2.20
Leu 13	9.62 ± 0.38	5.47 ± 0.22	24.6 ± 14.4	6.03 ± 3.52
Asn 87	373 ± 49.6	7.65 ± 1.02	204 ± 10.1	7.29 ± 0.36
Phe 122	9.23 ± 1.35	5.44 ± 0.79	9.79 ± 4.60	5.48 ± 2.58
Leu 10	3.48 ± 0.38	4.86 ± 0.53	7.59 ± 3.78	5.33 ± 2.65

residue	APH-Kan-Ternary		APH-Neo-Ternary	
	$P$ ( $\times 10^3$ )	$\Delta G_{\text{ex}}$ (kcal/mol)	$P$ ( $\times 10^3$ )	$\Delta G_{\text{ex}}$ (kcal/mol)
Ile 247	6.90 ± 0.96	5.27 ± 0.73	23.5 ± 13.9	6.00 ± 3.55
Leu 13	8.43 ± 1.78	5.39 ± 1.14	25.0 ± 1.03	6.04 ± 0.25
Phe 122	29.7 ± 7.23	6.14 ± 1.50	25.4 ± 7.07	6.05 ± 1.68

<sup>a</sup> See Materials and Methods for calculation details. Reported errors are from exponential decay curve fitting.

peaks indicating a small range of differing chemical environments for each backbone amide. This suggests that the apoenzyme may adopt multiple conformations with intermediate interconversion rates that would drastically broaden the signals. In either case, this provides an inherent flexibility that is likely the property utilized for broad aminoglycoside promiscuity. Hydrogen–deuterium exchange studies reveal that after only 15 min of exposure to D<sub>2</sub>O, less than 20% of all backbone amide resonances remain in the spectrum. These peaks gradually decrease in intensity until all are completely dissipated to noise level at 15 h (Figure 2A).

In the presence of the MgATP analogue, MgAMPPCP, the HSQC<sub>H2O</sub> spectrum has very little peak dispersion reminiscent of apo-APH (Figure 1B). However, upon close inspection, the nucleotide-bound form actually has a *lesser* distribution of isolated, distinguishable resonances although approximately 5% of the backbone amide groups remain protected from solvent up to 95 h of exposure to D<sub>2</sub>O (Figure 2B). Identities of these few resonances are not known because, unlike enzyme–aminoglycoside complexes, the overlap observed in HSQC spectra of the apo-APH and enzyme–MgAMPPCP render these spectra unsuitable for resonance assignments of a protein of this size. Chemical shift mapping experiments were also unsuccessful to allow assignments from the enzyme–tobramycin complex to be carried over to these spectra.

**Antibiotic Binding.** When APH is in a binary complex with antibiotic, the HSQC<sub>H2O</sub> spectrum undergoes a dramatic alteration relative to that for the apoprotein (Figure 1C).<sup>11</sup> Although there are antibiotic-dependent differences in all cases, about 85% of all nonproline resonances move to well-isolated positions with proton chemical shifts between 6 and 11 ppm in the binary APH–aminoglycoside complexes, while the majority of those in the apoenzyme range from only ~7.5–8.8 ppm. This indicates that APH adopts a well-defined structure upon binding of aminoglycosides.

Because of the broad substrate selectivity demonstrated by APH, it was of interest to determine specific residues affected by binding to two structurally diverse aminoglycosides. To this end, HSQC<sub>H2O</sub> spectra were acquired for the APH–kanamycin and APH–neomycin complexes where it was observed that more than 40 residues display significantly different cross-peak positions. Several of these are illustrated in Figure 3. Further-

more, HD exchange data revealed at least 20 backbone amides with much greater solvent protection for neomycin-bound APH relative to kanamycin (Figure 3, green colored residues). Only one of the residues (Arg 226) with chemical shift and solvent protection differences are within 4.5 Å of the bound aminoglycoside, while the rest are scattered in positions distal to the antibiotic binding site (>8 Å). The phenomenon of a large number of amides with chemical shift differences between complexes of enzyme with aminoglycosides is not limited to structurally different aminoglycosides but were also observed between complexes of structurally very similar aminoglycosides such as kanamycin A and kanamycin B (data not shown). These observations clearly indicate that effects of ligand binding to APH on structural and dynamic properties of this enzyme are not limited to changes in the active site only and are different for each ligand.

**APH–Nucleotide–Antibiotic Complexes.** HD exchange patterns in APH–kanamycin–MgAMPPCP and APH–neomycin–MgAMPPCP complexes, which represent APH with all bound substrates, were also determined. For simplicity, these complexes will be referred to as ternary forms of the enzyme henceforth.

When the HSQC spectrum of binary APH–kanamycin is compared to that of its ternary, it becomes apparent that ~30 cross-peaks present in the binary complex are absent in the ternary complex. This is attributable to line broadening from intermediary chemical exchange rates of these resonances. Amino acids to which these resonances belong are situated in and around the nucleotide binding site (Figure 4).

Complementary to these results, HD exchange shows a dramatic *increase* in solvent accessibility of >20 unbroadened residues in the presence of nucleotide (Figure 2C, D). Again, the vast majority of these are situated near the APH–nucleotide interface.

For the APH–neomycin ternary complex, only five residues demonstrate line broadening (Figure 4-green). These five are common among both ternary complexes studied and include Ala 93, Lys 44, Leu 33, Val 20, and one residue yet to be assigned firmly. Moreover, only 10 unbroadened residues display a significant enhancement in HD exchange upon the formation of the neomycin ternary complex as compared to more than 20 observed with kanamycin. Tyr 42, Met 45, and Thr 46 are among those residues that undergo a dramatic increase in HD exchange in the neomycin ternary complex. Interestingly, these three are listed with those broadened (missing) resonances due to nucleotide binding to the APH–kanamycin complex. Note that Lys 44, whose peak is missing in both ternary complexes, is a sequential neighbor whose side chain is shown to make direct contact with the nucleotide.<sup>14</sup> All of these residues are of exceptional significance because their amide protons are involved in interstrand hydrogen bonds of the five stranded, antiparallel β-sheets located at the nucleotide binding interface.<sup>14,15</sup>

Val 57 and Glu 60 also show increased HD exchange in the neomycin ternary complex, while these are line broadened in the kanamycin ternary. These residues are located within an α-helix close by the β-sheet discussed above. It has been shown that Glu 60 forms a stabilizing electrostatic interaction with Lys 44 that allows the lysine to be more stable for nucleotide coordination in the active site.<sup>14</sup> According to the crystal structure, one face of this α-helix makes extensive hydrophobic interactions with two strands of the β-sheet. Taken together, these data suggest that many of the hydrogen bonds involved in formation of the β-sheet and α-helix are either weakened or

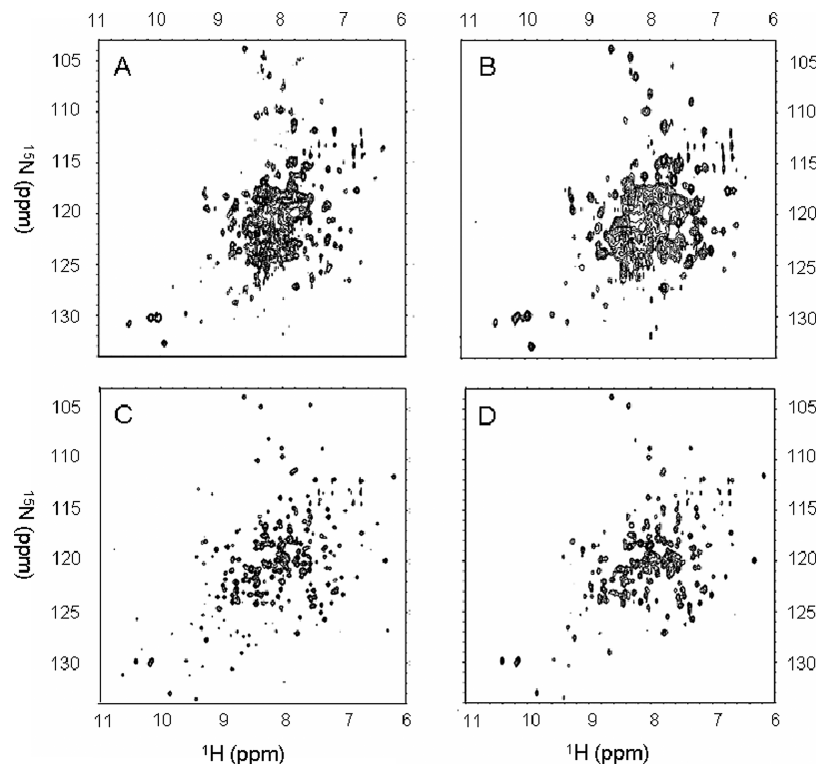


**Figure 1.**  $^1\text{H}$ - $^{15}\text{N}$  HSQC<sub>D2O</sub> spectra for ligand-free and ligand-bound forms of APH. (A) apo-APH; (B) APH-MgAMPPCP; (C) APH-Kanamycin and (D) APH-Kanamycin-MgAMPPCP. All are at matching contour levels.

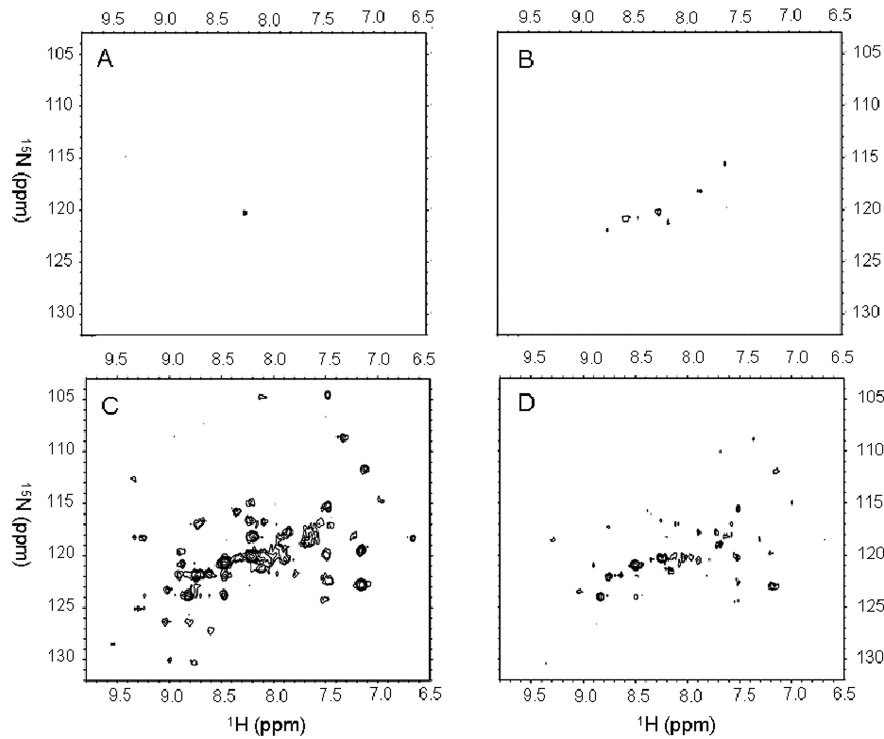


**Figure 2.** HD exchange in apo-APH and various APH-ligand complexes detected by  $^1\text{H}$ - $^{15}\text{N}$  HSQC<sub>D2O</sub> experiments. (A) apo-APH at  $t = 900$  min; (B) APH-MgAMPPCP at  $t = 3195$  min; (C) APH-Neomycin at  $t = 3195$  min; and (D) APH-Neomycin-MgAMPPCP at  $t = 3195$  min. All are at matching contour levels. Differential exchange patterns between binary and ternary APH-neomycin observed in the spectra of panels C and D are similar for kanamycin-bound complexes of APH.

broken as a result of nucleotide binding and may help explain the large difference in previously observed global thermodynamic parameters of binary versus ternary complexes as will be discussed in a later section.

**Rates of Exchange.** HD exchange patterns of amides are broadly divided in three categories determined by the length of time in which the amide peak remains in the spectrum after  $\text{D}_2\text{O}$  exposure: fast exchange ( $\leq 3\text{--}4$  min), intermediary ex-

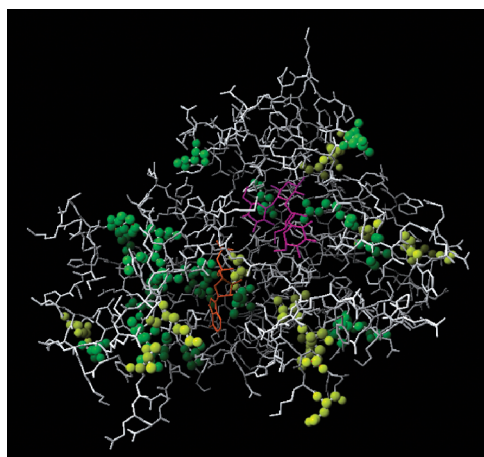


**Figure 3.** Residues differentially affected by binding of kanamycin and neomycin to APH. Residues with differentially altered chemical shifts and solvent accessibility are illustrated in yellow and green, respectively. Neomycin is shown in purple and ADP in orange for reference. Protein data bank identification number 2B0Q.

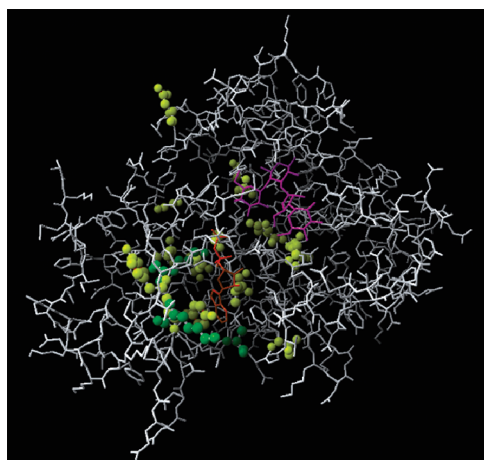


**Figure 4.** Residues with line broadening upon addition of MgAMPPCP to the APH–aminoglycoside complex. Shown in yellow are those found only when kanamycin is the antibiotic substrate, while green amino acids are common to both kanamycin and neomycin APH complexes. Neomycin is shown in purple and ADP in orange for reference. Protein data bank identification number 2B0Q.

change (4 min to 36 h), and slow exchange ( $\geq 36$  h). The criteria for slow exchange are based on the observation that little change occurs in the spectrum beyond 36 h regardless of complex. An intermediary exchange minimum of 4 min is selected because this is the experimental dead time prior to acquisition of the first NMR spectrum (see Materials and Methods).

Quantitative HD exchange rates of only a few backbone amides were determined because (1) a great number ( $\geq 60\%$ ) of amide protons exchanged before the first spectrum could be acquired (are in fast exchange); (2) the slowest exchanging residues, accounting for 20–30% of resonances depending upon the APH complex in question, did not display a measurable decrease in intensity within the time frame of the experiments ( $\sim 95$  h); and (3) a number of the remaining resonances were either in overlapping regions or their intensity was too weak for accurate integration. Thus, depending upon the complex, between 9 and 18 residues out of an initial  $\sim 250$  had calculable exchange rates, and only a few of these are common among the complexes studied. Exchange rates and derived thermodynamic parameters of the backbone amides that are shared

between various enzyme–ligand complexes are listed in Table 1. We emphasize that conclusions presented in this text are not dependent upon the quantitative analysis of these residues but rather on the unique behavior of various amino acids in different complexes that highlight differential dynamics of APH–ligand interactions.

## Discussion

**Apo-APH Has an Unusually Dynamic Backbone.** In the absence of ligands, the HSQC spectrum of APH shows significant resonance overlap with the vast majority of peaks situated between  $\sim 7.5$  and 8.8 ppm in the  $^1\text{H}$  dimension.<sup>11</sup> This is common for denatured or partially unfolded proteins.<sup>25–27</sup> Data acquired with circular dichroism spectroscopy (unpublished, Ozen and Serpersu) and the crystal structure<sup>14</sup> show that extensive secondary structure exists in apo-APH. From this, it is plausible that the apoenzyme is natively in a conformational state where the secondary structure has formed, but hydrophobic interactions that aid in tertiary structure are weak. As a result, APH is likely to be highly flexible, sampling several conformational states and thus creating broadened and overlapped amide resonances. Intuitively, this will produce a highly dynamic and potentially unstable overall protein structure. To test these hypotheses, NMR hydrogen–deuterium exchange experiments were conducted to qualitatively determine the dynamics of APH in the absence of ligand. Under our experimental conditions, over 80% of the backbone amide protons are exchanged for deuterium within 15 min of exposure to  $\text{D}_2\text{O}$  and after only 15 h, *every* amide hydrogen exchanges. Observation of a complete exchange of backbone protons of a 31 kDa protein in native form within such a time frame is quite rare. To our knowledge, there are no other examples of complete exchange except in cases of protein unfolding as seen for the apo-Src SH3 domain.<sup>28</sup> Such rapid and extensive exchange is indicative of a highly dynamic protein structure where hydrophobic cores and hydrogen bonds involved in secondary structure may be transient. We believe this to be one of the main reasons why this enzyme is so promiscuous in substrate selection and able to bind structurally diverse aminoglycosides with similarly favorable thermodynamic parameters.<sup>6,11</sup> A significant number of other proteins have been found to naturally exist in an intrinsically unfolded form and are induced to a defined structure upon ligand binding.<sup>29,30</sup> The inherent flexibility associated with such proteins is often a property utilized for broad substrate selectivity.

Crystallographic studies<sup>14,15</sup> report that the structure of APH is largely unaffected by substrate binding with the exception of the nucleotide and antibiotic positioning loops. Superpositioning the backbone of APH in several complexes yields rmsd values between 0.68 Å and 1.10 Å with the smallest deviation between APH–nucleotide and APH–nucleotide–kanamycin complexes while the largest is observed between apoenzyme and enzyme–nucleotide complexes. However, the NMR data presented in this work demonstrate that dynamic and structural features of the apoenzyme and aminoglycoside-bound forms are signifi-

- (25) Yao, J.; Dyson, H. J.; Wright, P. E. *FEBS Lett.* **1997**, *419*, 285–289.
- (26) Bai, Y. W.; Chung, J.; Dyson, H. J.; Wright, P. E. *Protein Sci.* **2001**, *10*, 1056–1066.
- (27) Mohana-Borges, R.; Goto, N. K.; Kroon, G. J. A.; Dyson, H. J.; Wright, P. E. *J. Mol. Biol.* **2004**, *340*, 1131–1142.
- (28) Wildes, D.; Marqusee, S. *Protein Sci.* **2005**, *14*, 81–88.
- (29) Wright, P. E.; Dyson, H. J. *J. Mol. Biol.* **1999**, *293*, 321–331.
- (30) Galea, C. A.; Wang, Y.; Sivakolundu, S. G.; Kriwacki, R. W. *Biochemistry* **2008**, *47*, 7598–7609.

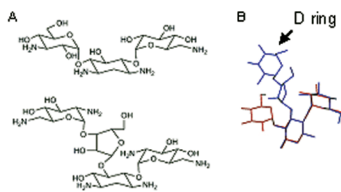


**Figure 5.** Structures of kanamycin A (panel A, top) and neomycin B (panel A, bottom). A 3D overlay of enzyme-bound conformations (panel B) demonstrates the differences in spatial orientation of the two aminoglycosides bound to APH where blue is neomycin and red is kanamycin.

cantly different in solution. The apoenzyme and the enzyme–nucleotide complex appear to have a distribution of interconverting conformations, whereas APH–aminoglycoside complexes display a well-defined structure. In addition, more than 15% of the cross-peak positions of residues throughout the protein can differ significantly between different enzyme–aminoglycoside complexes, depending upon the antibiotic bound, thereby further highlighting the dynamic nature of this protein.

**Neomycin Stimulates Greater Backbone Solvent Protection and Stability than Kanamycin.** For binary and ternary complexes of both kanamycin and neomycin, it is observed that at least 60% of the residues become solvent exchanged during the experimental dead time. However, the backbone amide protons of several amino acids are significantly less accessible to solvent (in slow exchange) when neomycin is the substrate but exchange fast when kanamycin is the bound ligand. Only one of these residues is in proximity to the antibiotic (Arg 226), while the rest are in distal regions (Figure 3). This is similar to observations made with the AKAP binding protein.<sup>31</sup>

What stabilizing interactions are present for the APH–neomycin complex that are absent for APH–kanamycin? We note that these two antibiotics differ in structure and spatial orientation. For neomycin, the 2-deoxystreptamine (DOS) ring common to all aminoglycosides is 4,5-disubstituted and contains four rings, whereas kanamycin is 4,6-disubstituted and has only three rings as illustrated in Figure 5. An overlay of enzyme-bound conformations<sup>32</sup> of these two aminoglycosides is also shown in Figure 5. The APH–neomycin–MgADP and APH–kanamycin–MgADP crystal structures<sup>15</sup> reveal that the amino acids with decreased solvent accessibility due to neomycin, in both binary and ternary complexes, are located in two regions of the protein. The first contains residues on the antibiotic binding domain in the region nearest the D ring of neomycin. This part of the protein maintains extensive hydrophobic interactions between several  $\alpha$ -helical moieties. Several residues that have significantly different chemical shifts between kanamycin and neomycin HSQC<sub>H2O</sub> spectra are also situated in this area (Figure 3). From the crystal structure, it is evident that only one interaction exists in this region between neomycin and APH that is not possible for kanamycin. Specifically, the hydroxyl at C3 of neomycin's D ring forms a hydrogen bond with Glu 231. This in itself may not suffice as an explanation for our data; however, because of the close association of the helical side chains, it is possible that this hydrogen bond could be the initiation of a chain of events leading to the observed ligand specific differences in this area.

The rest of the residues which significantly differ in HD exchange behavior between the kanamycin- and neomycin-

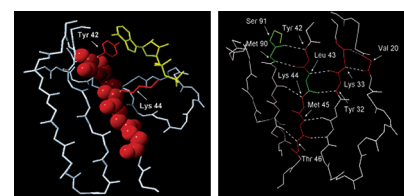


**Figure 6.** Nucleotide binding site of APH. (Left panel) Exchange-broadened residues on the  $\beta$ -sheet of the APH–neomycin ternary spectrum are shown in red. Lysine 44 and tyrosine 42 are shown with their side-chain interactions with ADP (yellow). (Right panel) Amino acids with an increase in solvent accessibility due to nucleotide binding are shown in green amidst those that demonstrate line broadening in the APH–neomycin ternary spectrum (red). For clarity, only the hydrogen bonds relevant to the discussion are shown.

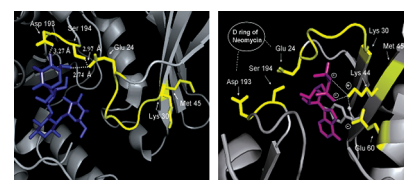


**Figure 7.** (Left panel) Interactions that involved in enhanced structural and dynamic stability of APH induced by neomycin binding. Shown interactions of the 4'' hydroxyl and 6'' amine groups of ring D of neomycin with APH are exclusive to neomycin due to the absence of this ring in kanamycin. (Right panel) Nucleotide interactions with Lys 44 and Tyr 42 (shown in gray for clarity) counteracts some of the stabilization effects of neomycin binding.

bound forms of the enzyme are located in the antiparallel  $\beta$ -sheet and the nearby  $\alpha$ -helix located on the nucleotide binding domain. In the absence of nucleotide, Lys 44, Met 45, Thr 46, Glu 60, and Trp 85 slowly exchange when neomycin is present but are in a fast exchange regime with kanamycin (Figure 6B). Of these, only Lys 44 displays broadening behavior for the neomycin-bound ternary complex. However, Lys 44, Met 45, Thr 46, and Glu 60 are all broadened in the ternary complex with kanamycin. This indicates that the noncovalent interactions of the enzyme to both nucleotide and antibiotic contribute to the stability of the  $\beta$ -sheet and its neighboring helix. In other words, ATP binding induces some destabilizing effects (to be discussed in a later section) while neomycin propagates counteracting associations that kanamycin is not capable of.

It is not straightforward to explain how neomycin causes such changes in solvent accessibility in this region. However, we propose that an intricate series of interactions are induced by formation of a hydrogen bond between the 4'' hydroxyl of neomycin ring D with the carboxyl side chain of Asp 193 located on a nearby loop. This stabilizes the loop which in turn allows for a subsequent hydrogen bond to take place between the side chains of Ser 194 (of the same loop as Asp 193) and Glu 24 situated on the nucleotide positioning loop. In addition, the 6'' amine of neomycin forms an electrostatic interaction with Glu 24. Lys 30 is seated at the apex between the newly stabilized nucleotide positioning loop and one of the strands of the  $\beta$ -sheet. The backbone carboxyl group of Lys 30 forms an interchain hydrogen bond with the backbone amide of Met 45 in the  $\beta$ -sheet. A schematic of these interactions is presented in Figure 7. Kanamycin, lacking a fourth ring and any similar contacts, is unable to facilitate such stabilizing propagation.

Ligand-induced transmission effects are not uncommon. For example, an intricate network of hydrogen bonds through a series of water molecules was found through HD exchange to be responsible for heme oxygenase plasticity and propagating

(31) Fayos, R.; Melacini, G.; Newlon, M. G.; Burns, L.; Scott, J. D.; Jennings, P. A. *J. Biol. Chem.* 2003, 278, 18581–18587.  
(32) Owston, M. A.; Serpersu, E. H. *Biochemistry* 2002, 41, 10764–10770.

the effects of ferric azide and cyanide binding.<sup>33</sup> Similarly,  $\alpha$ -helices and  $\beta$ -strands are stabilized by both direct and indirect ligand contact in dihydrofolate reductase complexes.<sup>34</sup> These interpretations reiterate the incredible complexity of protein–ligand interactions.

**Binding of Nucleotide Increases Backbone Solvent Accessibility and Structural Flexibility of the Nucleotide Binding Region.** Direct comparison of the APH–kanamycin binary and ternary spectra reveals that approximately 30 cross-peaks found in the binary complex become exchange broadened and NMR undetectable when metal–nucleotide is added. Not surprisingly, the residues belonging to those resonances are found to be concentrated around the nucleotide binding site (Figure 4). This is also the case when neomycin is the antibiotic although only five residues are missing from the ternary spectrum in this case. The likely cause for this dramatic difference between the complexes formed in the presence of kanamycin and neomycin is an increase in structural stability found for neomycin-bound APH as discussed earlier.

One might argue that the missing resonances may have simply shifted underneath other peaks or into a crowded region. However, there are 30 absent peaks in the kanamycin ternary spectrum, while all other peaks have a corresponding binary resonance with no significant changes in chemical shifts. Therefore, it is unlikely that so many resonances could all have become “hidden”. A similar situation of broadening is found when subtilisin complexes with prodomain, resulting in a loss of HSQC peaks.<sup>35</sup>

Several of the broadened peaks observed in the APH ternary complexes belong to residues involved in the interstrand hydrogen-bonding network facilitating the formation and stability of a five-stranded, antiparallel  $\beta$ -sheet. These include Val 20, Tyr 32, Lys 33, Tyr 42, Lys 44, Met 45, and Thr 46 in the kanamycin ternary complex, while only Val 20, Lys 33, and Lys 44 are broadened for the neomycin ternary (Figure 4). The side chains of Lys 44 and Tyr 42 from the  $\beta$ -sheet directly interact with nucleotide via a salt bridge/hydrogen bond and a  $\pi$ – $\pi$  ring-stacking interaction, respectively.<sup>14,36,37</sup> Moreover, Val 57 and Glu 60, located on the nearby  $\alpha$ -helix, are broadened in the kanamycin ternary complex and not in neomycin ternary. Glu 60 forms an electrostatic interaction with Lys 44 on the  $\beta$ -sheet. This helps position the Lys 44 side chain for contact with the phosphate groups of the incoming nucleotide. It appears, then, that nucleotide binding causes a disruption or weakening of the natural hydrogen bonding between some of the backbone amide protons and their carbonyl partners. Therefore, it is likely that association of the side chains of Lys 44 and Tyr 42 with nucleotide causes the sheet to stretch or buckle at the areas of contact subsequently weakening their interstrand hydrogen bonds (Figure 5, right, and Figure 6). While other examples of increases in exchange upon ligand binding exist in literature,<sup>34,38</sup> the molecular bases for such phenomena have not been discussed.

(33) Rodriguez, J. C.; Wilks, A.; Rivera, M. *Biochemistry* **2006**, *45*, 4578–4592.

(34) Polshakov, V. I.; Birdsall, B.; Feeney, J. *J. Mol. Biol.* **2006**, *356*, 886–903.

(35) Sari, N.; Ruan, B.; Fisher, K. E.; Alexander, P. A.; Orban, J.; Bryan, P. N. *Biochemistry* **2007**, *46*, 652–658.

(36) Boehr, D. D.; Farley, A. R.; Wright, G. D.; Cox, J. R. *Chem. Biol.* **2002**, *9*, 1209–1217.

(37) Thompson, P. R.; Boehr, D. D.; Berghuis, A. M.; Wright, G. D. *Biochemistry* **2002**, *41*, 7001–7007.

(38) Lee, T.; Hoofnagle, A. N.; Resing, K. A.; Ahn, N. G. *J. Mol. Biol.* **2005**, *353*, 600–612.

Further evidence of a  $\beta$ -sheet destabilization comes from evaluation of the HD exchange data for APH–antibiotic complexes in the absence and presence of MgAMPPCP. Of the residues in the  $\beta$ -sheet that have analyzable peaks in both binary and ternary spectra for kanamycin-bound APH, several are characterized by slow exchange (strong protection from solvent) in the absence of nucleotide and then move into a fast exchange regime when MgAMPPCP is present. Included in this category are Leu 43, Met 90- and Ser 91. From Figure 6B it is clear that these residues (green) are each within the regions of the amino acids with nucleotide-induced resonance broadening (red) and with the exception of Ser 91 are hydrogen bond partners with each other.

In the neomycin ternary complex, many of the residues that are exchange broadened in the kanamycin ternary complex, including Tyr 42, Met 45, Thr 46, and Glu 60, are in slow exchange in neomycin binary but quickly exchange with solvent in the presence of nucleotide. This emphasizes the conclusion that neomycin induces greater protein stability than kanamycin and that nucleotide binding counteracts some of these effects (Figure 5).

The increased solvent accessibility and change in  $\beta$ -sheet stabilization becomes even more significant when the side-chain blocking effect is considered. Bai and Englander<sup>39</sup> demonstrated that amino acids in  $\beta$ -sheets having long side chains can protect the backbone from solvent, resulting in an *increase in the strength of the interstrand hydrogen bonds*. This is relevant to APH in that the side chains of the  $\beta$ -sheet that point toward the solvent where nucleotide interactions include those with leucines, methionines, tyrosines, and lysines (Figure 6B). The opposite side of the  $\beta$ -sheet is protected from solvent by hydrophobic interactions with the N-terminal  $\alpha$ -helix. From this it could be postulated that, in the absence of nucleotide, solvent protection of the  $\beta$ -sheet amino acids occurs via side-chain blocking, with a greater protection with neomycin than kanamycin as previously discussed. When nucleotide binds, water molecules associated with the incoming nucleotide and/or at the binding interface may be trapped, creating an environment where the interstrand hydrogen bonds are weakened by being forced into interactions with solvent. This is supported by the fact that several of the residues undergoing exchange broadening in the presence of nucleotide are either in a slow or intermediary HD exchange regime in its absence as mentioned previously. One alternative explanation is that nucleotide interaction with Tyr 42 and Lys 44 causes the  $\beta$ -sheet to stretch or buckle at the point of contact, thus exposing the backbone amide groups of nearby residues to solvent and increasing the chances for an exchange event.

It is also suggested from the crystal structure that the backbone amide hydrogen of Ala 93, situated on a loop near the  $\beta$ -sheet, is directly involved in binding and stabilization of the adenine ring of ATP.<sup>14</sup> Intuitively, this proton will be more protected from solvent in the presence of nucleotide. In both the APH–kanamycin and APH–neomycin binary complexes, Ala 93 quickly exchanges within 4 min of D<sub>2</sub>O exposure as expected. However, this residue is among those amino acids with broadened resonances in both ternary complexes of APH, confirming the formation of a hydrogen bond with nucleotide.

Overall, an *increase* in solvent accessibility is observed for the nucleotide-bound APH–antibiotic complexes. The vast majority of amino acids displaying this property are restricted

(39) Bai, Y. W.; Englander, S. W. *Proteins* **1994**, *18*, 262–266.

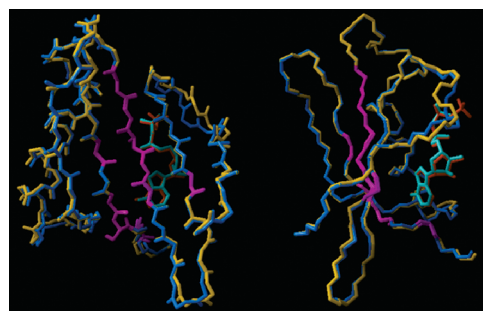


**Figure 8.** Front (left) and side (right) view of superimposed crystal structures of APH–MgAMPPNP<sup>14</sup> (yellow with red nucleotide) and APH–MgADP-kanamycin<sup>15</sup> (blue with cyan nucleotide) at the nucleotide binding region. Amino acids that are either broadened or show altered HD exchange patterns upon addition of nucleotide to the enzyme–aminoglycoside complex are shown in purple. Carbonyl oxygens are hidden in the right panel for clarity.

to the nucleotide binding site. Furthermore, a significantly smaller number of residues have calculable exchange rates in ternary complexes when compared to binary. While our dynamic data can be interpreted with the visual aid of the crystal structures, the observed ligand-induced differences are not readily visible in the structures themselves. When the  $\beta$ -sheet from crystal structures of apo- and ligand-bound APH is superimposed, rmsd values between 0.21 Å and 0.56 Å are observed. An example is shown in Figure 8 as an overlay of the binary APH–nucleotide with the ternary APH–nucleotide–kanamycin complexes.

Our data also provide rationale for the significant differences observed between the global thermodynamic parameters of binary and ternary complexes where the formation of ternary complexes were accompanied by significantly less negative enthalpy (by more than 15 kcal/mol) than binary complexes,<sup>6</sup> which was compensated by a more favorable entropy yielding similar  $\Delta G$  values for both types of complexes. From results described in this paper, it is possible to attribute the less negative  $\Delta H$  of the ternary complex, at least in part, to the weakening/breaking of the hydrogen bonds of the  $\beta$ -sheet and the neighboring  $\alpha$ -helix. The resulting decrease in stability of the  $\beta$ -sheet and its immediate surroundings may contribute to the observed increase in entropy. Release of some solvent molecules upon binding of nucleotide may also contribute to increased entropy observed for the formation of ternary complexes. Osmotic stress experiments to determine the extent of solvent release upon binding were unsuccessful because of the

tendency of this protein to interact differentially with varying osmolytes, thus providing inconclusive data.

### Conclusions

In this work, we described APH–ligand interactions in an amino acid-specific manner in analysis of dynamic properties of an aminoglycoside-modifying enzyme for the first time. Here we provide further evidence for an inherently very flexible apoenzyme as the means for broad substrate promiscuity. Our data show that antibiotic binding alters dynamic properties of the enzyme and induces a well-defined protein structure in an antibiotic-dependent manner. Specifically, neomycin increases the dynamic and structural stability of APH relative to kanamycin. This complements our previous observation of dramatic differences between complexes of kanamycins and neomycins with APH regarding solvent effects as well as in heat capacity ( $\Delta C_p$ ).<sup>11</sup> In that work, we attributed the very large decrement in the heat capacity to conformational changes in the protein which are now supported by HD exchange data. Furthermore, nucleotide interaction with APH does not appear to significantly alter APH structure but in fact *increases* solvent accessibility at the nucleotide binding site and weakens interstrand hydrogen bonds in the nearby  $\beta$ -sheet and  $\alpha$ -helix.

Our data support the hypothesis that APH is designed to recognize aminoglycosides and it is the noncovalent interactions of APH with antibiotic and not nucleotide that are required to induce a stable and well-defined enzyme structure in solution. It is plausible that this is one of the evolutionary means by which APH is geared to respond to the ever changing flux of aminoglycoside antibiotics. These properties, in conjunction with a high concentration of negatively charged side chains in the active site that is similar to RNA, the natural aminoglycoside target, allow APH to detoxify a large number of structurally diverse aminoglycoside antibiotics. Overall, our results aid in understanding detailed protein–ligand associations for APH that may be applied to other aminoglycoside-modifying enzymes and/or highly promiscuous proteins in general.

**Acknowledgment.** This research was partly supported by a Grant from the National Science Foundation (MCB 01110741 to EHS) and the Center of Excellence for Structural Biology at the University of Tennessee. We thank Can Ozen for purification of isotopically labeled APH. We also thank Dr. Elias Fernandez for critical reading of the manuscript.

**Supporting Information Available:** This material is available free of charge via the Internet at <http://pubs.acs.org>.

JA901685H